Nanosecond Pulsed Laser Irradiation of Titanium Alloy Substrate: Effects of Periodic Patterned Topography on the Optical Properties of Colorizing Surfaces

J.M. Vazquez-Martinez [1],*[ID]**, J. Salguero** [1][ID]**, E. Blanco** [2][ID] **and J.M. González-Leal** [2][ID]

[1] Department of Mechanical Engineering & Industrial Design, Faculty of Engineering, University of Cadiz, Av. Universidad de Cadiz 10, E11519 Puerto Real-Cadiz, Spain; jorge.salguero@uca.es

[2] Department of Condensed Matter Physics, Faculty of Sciences, University of Cadiz, Av. República Saharui, E11510 Puerto Real-Cadiz, Spain; eduardo.blanco@uca.es (E.B.); juanmaria.gonzalez@uca.es (J.M.G.-L.)

* Correspondence: juanmanuel.vazquez@uca.es

Abstract: Most of the current works based on surface treatments of metals by laser marking technology are focused on the modification of the color tonality of flat surfaces, or the development of specific topography features, but the combination of both processes is not usually evaluated, mainly due to the complexity of controlling the optical properties on rough surfaces. This research presents an analysis of the influence of the micro-geometrical characteristics of periodic patterned laser tracks on the chromaticity and reflectance of Ti6Al4V substrates. The samples were irradiated with an infrared nanosecond pulsed laser in air atmosphere, taking as the control parameter the scan speed of the beam. A roughness evaluation, microscopic inspection, and absorption and chromaticity examination were conducted. Although micro-crack growth was detected in an isolated case (10 mm/s), the possibility of adjusting the result color was demonstrated by controlling the heat-affected zone thickness of the textures. The results of rough/colored combined textures allow new perspectives in industrial design to open, particularly in aesthetic applications with special properties.

Keywords: titanium; laser marking; color; reflectance; roughness; oxidation

1. Introduction

Surface texturing has recently grown in importance in engineering applications, resulting in significant improvements in load capacity, wear resistance, and the friction coefficient of tribo-mechanical parts. Under tribological conditions, texturing geometries remove wear debris from the sliding track, reducing the involved abrasive effects of these hard particles, and also acting as lubricant reservoirs [1,2].

Among the several techniques that can be applied for texturing (micro-drilling, mechanical indentation, electro-discharge texturing, etc.), laser surface texturing (LST) has shown some relevant advantages regarding chemical and mechanical processes. On the one hand, the laser system can be adapted to a wide range of parameters and become a faster and more flexible method than machining operations. On the other hand, these treatments are usually based on laser irradiation processes in air atmosphere, avoiding the use of lubricants or coolant fluids that is necessary in some machining processes [3].

Therefore, LST is considered as a viable process for surface engineering, contributing to the development of the functionalization of components [4]. It also contributes to the development of

sustainable manufacturing by means of an environmentally friendly process in comparison to chemical and conventional machining [5,6].

Ti_6Al_4V is a well-known $\alpha + \beta$ (grade 5) Ti-based alloy, widely used for the manufacturing of aerospace parts and biomedical components, mainly due to its good weight/mechanical properties ratio, high corrosion resistance, and excellent biocompatibility.

The ability to maintain control over the main mechanical properties on the surface of this alloy by LST can produce several benefits. In the healthcare sector, the biocompatibility and biomechanical behavior are key factors, as well as the improvement of the sliding features under biological fluids [7,8]. In the case of strategic alloys for the aerospace industry, surface modification treatments are used to overcome material limitations and to improve functional performance [9–11].

In the case of the Ti_6Al_4V alloy, the use of LST is focused to overcome functioning limitations such as poor wear behavior. The unstable frictional response of titanium alloys coupled with severe wear behavior under certain rubbing conditions make the use of this type of alloy difficult to apply in complex tribological applications [12,13]. The selection of parallel linear displacements aims to develop laser tracks that can be used as micro-channels for controlling the fluid distribution on the surface. This effect allows wear resistance to be improved under lubricated conditions of the substrate [14,15].

Moreover, the exposure of this alloy to LST treatment in an air atmosphere—favored by a local increase of temperature—causes the external surface layer to combine with the oxygen present [16], giving rise to the development of a thin protective layer composed of titanium oxides mainly in rutile (TiO_2) form [17,18].

After the phenomena of oxidation, transparent oxide films on a reflecting substrate give rise to color. Thus, titanium substrate reacts by changing the initial tonality to a color range mainly related to the thickness of the oxide layer and the conditions of the thermal treatment [19,20].

A wide range of color tonalities can be achieved by modifying the main control parameters of the LST process in Ti_6Al_4V, including variables such as thickness and microstructure of the oxidation layer [21].

The property of color can be considered as aesthetic or non-functional regarding the advantages that the LST process can provide, but can also be considered as an easy indicator of the characteristics of the treated surface. The kind of color can determine the surface characteristics. Additionally, by modifying parameters during the LST process, textures with color variations can be obtained, such as the color laser marking in steel [22].

There are several studies in the scientific literature that report the LST of the Ti_6Al_4V alloy. These are mainly focused on the characterization of micro-geometry and the study of the relationship with tribological behavior, which is generally evaluated by studying the wettability and surface roughness [2,4,6,14,23].

There are also some works that relate to the influence of LST parameters on the color of textured surfaces. These mainly evaluate the optical properties (n, k) of oxide films using spectrophotometry and ellipsometry techniques [24–29]. These measurements are useful for calculating spectral reflectance and can then be compared with the data measured by a spectroscope. The appearance of these titanium laser-grown oxide coatings is described by chromaticity, a standard by which these identifiers can be compared [30,31].

A lake of knowledge has been detected in the scientific literature about the study of color/mechanical properties and process parameters.

In this paper, a study of the chromatic changes—in terms of optical reflectance and chromaticity—and their relationship with micro-geometrical variations—in terms of roughness—is reported. LST parameters in the texturing of Ti6Al4V are key for the control of surface morphology, which can be directly linked with the chromatic state.

2. Materials and Methods

2.1. Laser Texturing Process

Ti6Al4V titanium alloy (UNS R56400) 50 mm × 50 mm plates with 5 mm thickness were cleaned with petroleum ether/ethanol 50% solution. These plates were conditioned by mechanical polishing to an initial surface roughness of Ra < 0.05 μm and Rz < 0.15 μm. The Ti6Al4V chemical composition (wt %) shown in Table 1 was evaluated by means of the optical emission spectroscopy (OES) technique using a SpectroMAX X system (SPECTRO Analytical Instruments GmbH, Kleve, Germany). With this technique, a comparison with certified substrate references was performed to obtain the sample composition of the Ti6Al4V.

Table 1. Experimental Ti6Al4V substrate composition (wt %).

Al	V	Fe	C	O	N	H	Ti
6.26	3.91	0.18	0.011	<0.10	<0.10	<0.10	Rest

Laser exposure was performed in room air atmosphere, using a commercial marking machine (ROFIN-SINAR Technologies Inc., Plymouth, MI, USA) based on a 10 W Ytterbium fiber infrared laser system with a $\lambda = 1070 \pm 5$ nm wavelength, which generates pulses of a $\tau = 100$ ns duration at a repetition rate of $f = 50$ kHz. The laser spot with a focal diameter of $d = 60$ μm was moved over the surface of the sample with a scanning speed (V_s) ranging from 10 to 300 mm/s. The texturing process was developed through bidirectional parallel lines with a 0.1 mm distance between the laser tracks. The textured areas over the Ti6Al4V substrate consisted of 10 mm × 10 mm size squares.

To evaluate the influence of laser processing parameters on the variation of the properties and features of the modified surfaces, the scanning speed of the beam (V_s) was taken as the control parameter. Under this assumption, a single energy density of pulse/fluence (E_d) was chosen for the experimental tests, combined with nine different values of V_s, which are shown in Table 2.

Table 2. Laser processing parameters.

Nominal Power (W)	Pulse Rate (KHz)	Single Energy Density of Pulse/Fluence (E_d) (J/cm^2)	Scanning Speed of Beam (V_s) (mm/s)								
10	50	7.07	10	25	50	75	100	150	200	250	300

2.2. Evaluation Methods

Textured samples were subjected to two different types of analysis, on the one hand, of the chromatic changes, and on the other hand of the micro-geometrical variations, in terms of roughness, all induced by the laser treatments.

Color modification of the surfaces was evaluated by measuring the optical reflectance of the samples using both a dispersive spectrophotometer (Agilent, model Cary 5000, Santa Clara, CA, USA) along with a 150 mm diameter integrating sphere accessory and a spectroscopic ellipsometer (Woollam, model VASE, East Brisbane, Australia). Optical geometries of 8°/di and 8°/de were used for color measurements, following the recommendations of the CIE (Commission Internationale de L'Eclairage, Vienna, Austria) [32] Light reflectance values (LRV) of the textured surfaces were determined following the recommendations of the British Standard [33,34].

For the study of micro-geometrical characteristics of the textures, a roughness measure device Mahr Perthometer Concept PGK120 (Mahr technology, Göttingen, Germany) was used.

Surface finish features were described by the roughness parameters of asymmetry or skewness (*Rsk*) and sharpness of the asperity peaks of kurtosis (*Rku*). These parameters, which are extracted

from the amplitude distribution curve (ADF), can provide valuable information about the shape of the laser tracks.

$$Rsk = \frac{1}{Rq^3}\left[\frac{1}{lr}\int_0^{lr} Z^3(x)dx\right] \tag{1}$$

$$Rku = \frac{1}{Rq^4}\left[\frac{1}{lr}\int_0^{lr} Z^4(x)dx\right] \tag{2}$$

R_q is a parameter that defines the root mean square roughness of the profile ordinates (Z) on the evaluation length (*lr*) [35]:

$$Rq = \sqrt{\frac{1}{lr}\int_0^{lr} Z^2(x)dx} \tag{3}$$

In addition to roughness characterization, laser tracks morphology and crack growth were studied on a cross-section of the grooves by means of optical and scanning electron microscopy methods. The influence of the laser processing parameters on the development of modified texturized layers was evaluated by measuring the hardness from the outer edge of the track. Under this consideration, the presence of oxidation phenomena, highly related with variations in color and hardness, was analyzed using energy dispersive X-Ray spectroscopy (EDX).

3. Results and Discussion

Laser texturing processes on the surface performs relevant modifications of the initial features of the substrate. The main alterations on the substrate can be related to micro-geometrical changes of the surface and color tonality variations of the samples. Due to the energy incidence of the laser along the paths used for this study, a material phenomenon occurred, allowing the development of a linear parallel pattern of grooves on the substrate to occur. Laser tracks showed specific combinations of shape and size as a function of the processing parameters. In the same way, microstructural and chemical composition variations were modified in the closest areas of the tracks, changing the initial properties of the titanium alloy. These kinds of modifications were easily detected due to color tonality variations.

3.1. Micro-Geometrical Morphology of the Laser Textures

In addition to the color variation, the modified samples showed a substrate removal process from the laser tracks. This removal process was caused by the development of a linear parallel pattern texture. However, the use of different processing parameters may have induced a wide range of shape and size of the grooves.

Taking as a reference the scanning speed of the beam, a decrease of the grooves depth as a function of Vs was detected. Affected Ti6Al4V debris deposited on the upper area of the tracks were noticed, meaning that the density chart showed two clearly differentiated areas of material (Figure 1). The analysis of the Rsk and Rku parameters showed significant differences between low, medium, and high Vs ranges.

For a lower scanning speed, an increase trend was detected on each studied roughness parameter. Based on the interpretation of the ISO 4287 and ASME B46.1 standards, higher values of Rsk > 0 implied that the laser tracks maintained a greater volume of material below the midline of the profile, which was understood as larger grooves caused by more aggressive treatments. For the Rku parameter, an increase trend with values greater than 3 were indicative of a sharp profile, confirming the existence of deep and narrow textures.
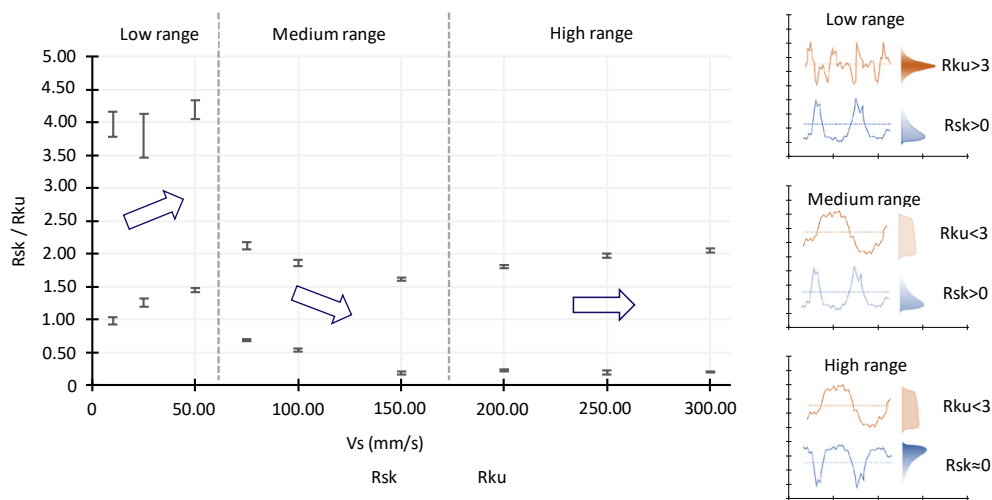
Figure 1. ISO 4287 asymmetry or skewness (Rsk) and sharpness of the asperity peaks of kurtosis (Rku) as a function of V_s.

Medium V_s ranges (75–150 mm/s) involved a decrease in the values of Rsk and Rku. This fact resulted in softer asperities caused by the laser beam, and lower depths of the tracks. From this V_s range, some material debris detachment was observed on the closest areas of the grooves.

The use of high ranges of V_s (200–300 mm/s) reduced the intensity of the treatments, giving rise to softer textures with low, deep, semicircular tracks. These treatments promoted the uniform behavior of the roughness values, with Rsk < 0.5 and Rku < 2.

Analysis of the probability density function (Adf) from the material ratio curve (BAC) of the measured profiles revealed the existence of two different curves based on the shape and size of the textures. On the one hand, from lower scanning speeds (10–50 mm/s), the BAC curve showed a single maximum in the Adf located in the midline of the roughness profile. Furthermore, when V_s increased, a displacement of the material below the midline was detected, as illustrated in Figure 2a. On the other hand, V_s ranges from 100 to 300 mm/s resulted in the generation of specific distributions, showing two maxima in the Adf located on both sides of the midline of the roughness profile (Figure 2b).
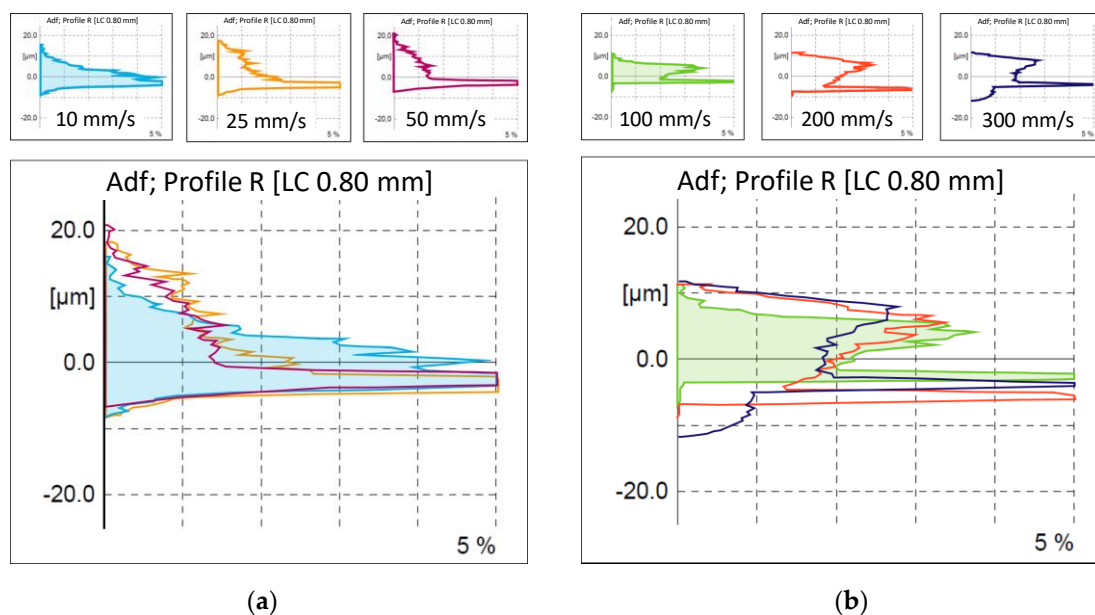

Figure 2. Different behaviors of the probability density function as a function of V_s. (Lc cut-off wavelength). (**a**) Single maximum Adf value, (**b**) Double maximum Adf values.

In addition to micro-geometrical modifications in terms of roughness, the LST treatments may have induced microstructure variations and oxidative phenomena on the modified layer.

3.2. Influence of LST on Heat-Affected Zone and Microstructure

As a consequence of the texturing process on the surface of the Ti6Al4V, microstructural changes were caused. A rapid temperature increase focused on small areas, and the cooling processes in the laboratory atmosphere may have affected the initial structure of the alloy. Furthermore, the development of the LST processes in room air atmosphere induced the presence of oxidative phenomena on the heat-affected zone (HAZ).

The Ti6Al4V (UNS R56400) alloy used for this research had an $\alpha + \beta$ equiaxed microstructure. However, the surface treatment and the introduction of oxygen (as an α-phase stabilized element) resulted in significant changes to the microstructure and mechanical properties of the alloy. As can be seen in Figure 3, the HAZ close to the texture tracks was highly influenced by the intensity of the treatment, quantified by the Vs.

As described, the HAZ showed an important dependence to the scanning speed of the beam. The increase of the Vs implies that the beam remained over the same section of the alloy for less time, giving rise to reduced tracks and consequently decreasing the HAZ, according to [17,35] (Figure 4).
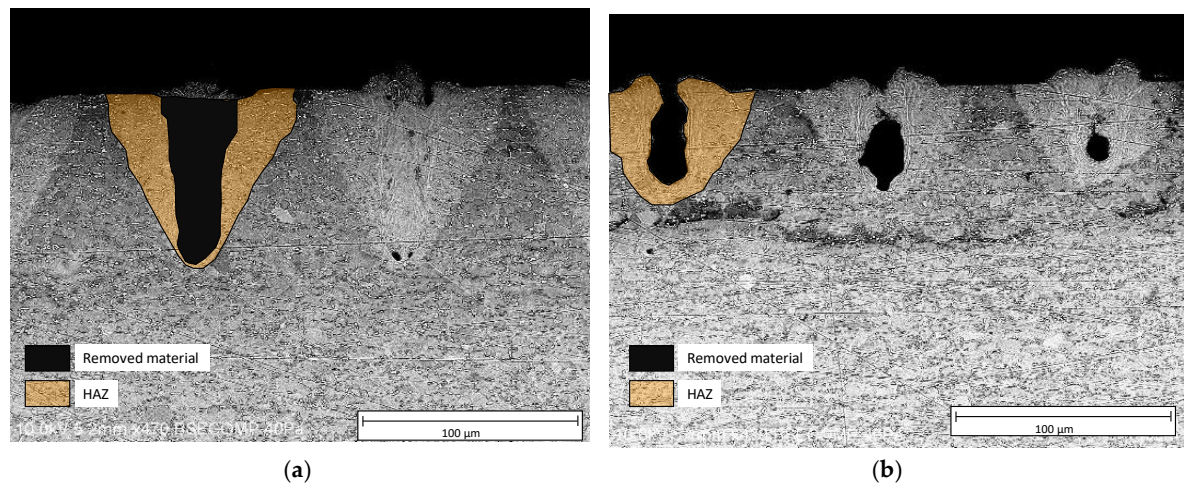

(**a**)   (**b**)

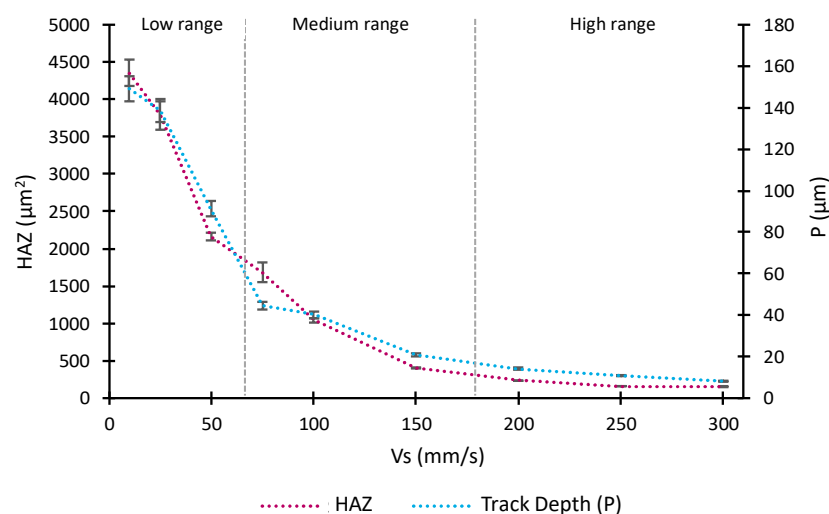**Figure 3.** Heat-affected zone of textured tracks (**a**) 50 mm/s; (**b**) 75 mm/s.

Figure 4. Heat-affected zone (HAZ) and depth of laser tracks as a function of V_s.

Regarding the microstructural modification, the rapid cooling process of the treated areas may have been the main cause of the transformation from equiaxed grains of an α+β to martensitic structures with laminar shape grains near to the α phase (Figure 5) in accordance with the results of [36].
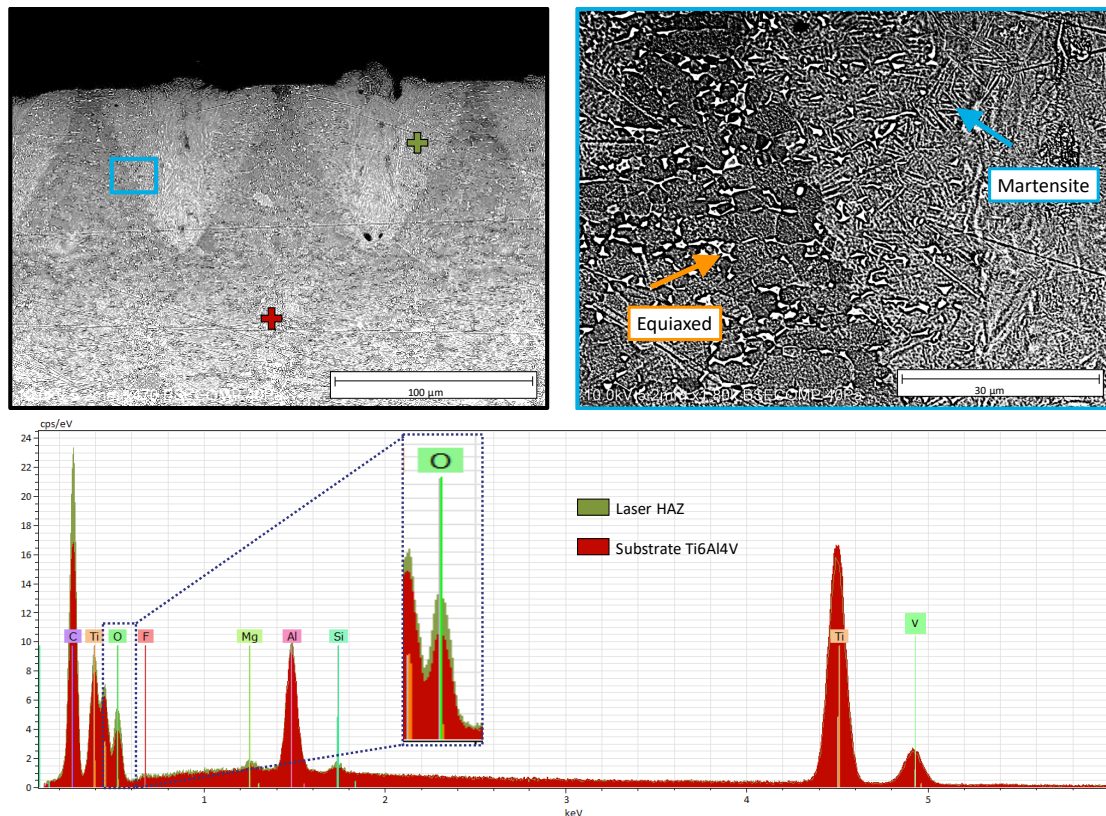

Figure 5. Microstructural and composition changes induced by laser treatment (V_s = 50 mm/s).

One of the most representative effects—in addition to the martensitic transformation—was the appearance of oxidative phenomena. This was mainly caused by the increase of the temperature in the air atmosphere, in which oxygen may have enriched the composition of the modified layer.

3.3. Hardness Variation and Crack Growth on Textured Surfaces

An increment in oxygen composition from the thermal oxidation, and the phase evolution to martensitic structure, made an increase of the hardness of the modified layer possible. By studying the hardness from the edge of the tracks, a direct relationship was observed between the scanning speed of the beam and the increase of hardness on the heat-affected zone. Under this consideration, the use of very low scanning speed (10 mm/s) had the best results in terms of the penetration ability of the treatment. Taking as a reference the hardness of the untreated substrate (Ti6Al4V) with a nominal value of approximately 349 Vickers Hardness (HV), by means of the laser surface treatments, a textured layer was obtained with a new hardness value more than four times higher than the initial one (Figure 6).

Using the high performance conditions for increasing the hardness (V_s = 10 mm/s), a maximum penetration range of 60 μm was determined through the measurement results to obtain significant mechanical improvements. Under this thickness, the laser treatment for this purpose may not be an effective method. On the other hand, mainly due to the cooling processes, in rare cases, the existence of micro-cracks may occur (Figure 6), according to [37]. Crack growth over the track surface is caused by the solidification process of the vaporized titanium alloy and the oxidation that takes place during the beam displacement.
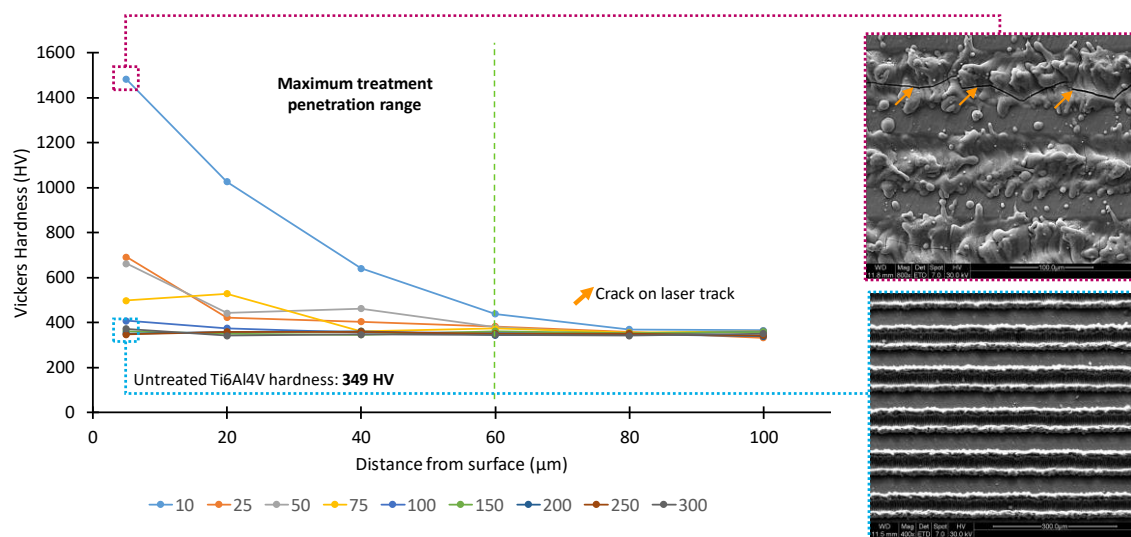
Figure 6. Hardness variation based on Vs and detail of laser track morphologies for 10 and 250 mm/s V_s.

3.4. Color Tonality Variation of Laser Textured Surfaces

Laser radiation treatments may affect both the micro-geometrical topography and the physicochemical properties of the surface. One of the most representative effects of the laser texturing process on the Ti_6Al_4V surface may be the color tonality variation. Under oxidation phenomena, the titanium substrate reacts, changing the initial tonality to a color range mainly related to the thickness of the oxide layer and the conditions of the thermal treatment.

When the tonality variations in the textures were analyzed, a sample color dependency was detected on the scanning speed of the beam. Under the range of V_s used, a color palette with golden and near-blue tones was developed (Figure 7). As was detected for previous parameters, the existence of three different ranges of V_s (low, medium, and high rates) also resulted in separate behaviors in terms of the development of color tonalities, in accordance with fluence groups [36].
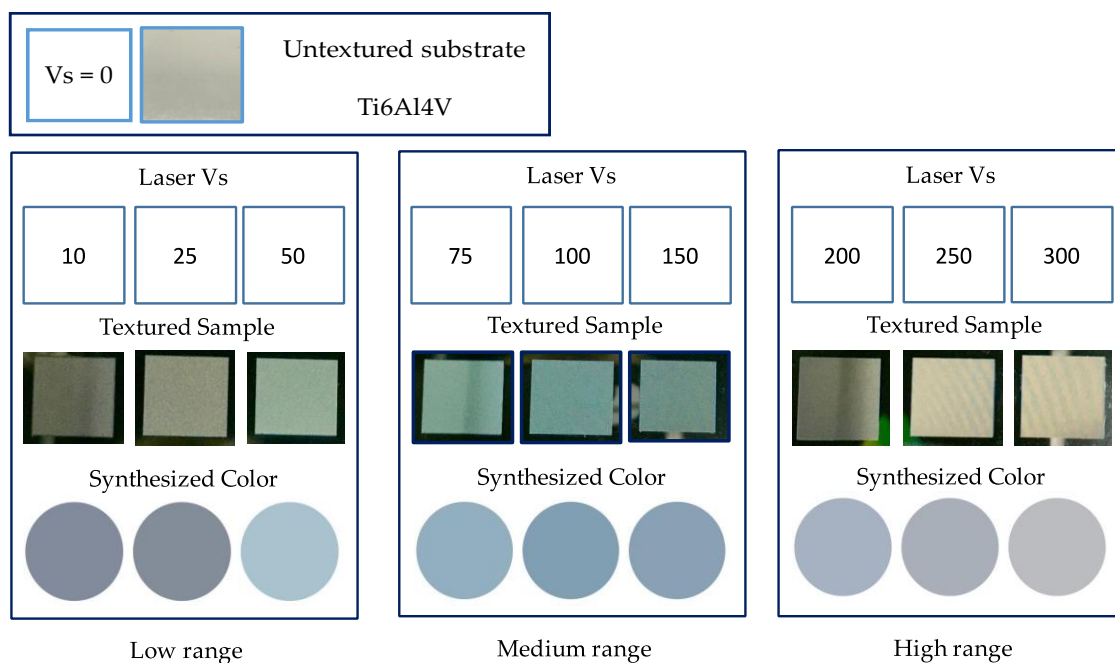

Figure 7. Color palette generated under different scanning speeds.

On these samples, the chromaticity coordinates $Y10x10y10$ were calculated from the reflectance spectra as measured with the integrating sphere and considering the standard colorimetry observer CIE1964 and the illuminant D65. Values of the $x10$ and $y10$ color coordinates for the samples under study are shown in the CIE1931 chromaticity diagram in Figure 8a.

A study of the different color coordinates revealed that the chromaticity coordinates ($X10y10$) were located in a small area on the center of the two dimensional diagram. This fact indicates a color locus quite reduced for this alloy and the parameters used in the study. However, through variations on the laser processing parameters, a wide variety in the color palette can be induced, according to [38].

The CIE 1931 color space ($x10$, $y10$, and $Y10$ (LRV)) indicated a singular point of the LRV value for a 50 mm/s scanning speed of the beam. This feature can be observed on the synthesized color image of the lower V_s range in Figure 7. Furthermore, a general growing trend was noticed for the color coordinate values ($x10$, $y10$) as a function of the V_s (Figure 8b). Likewise, the most intense colors of the laser texturing conditions that were used in this research were located under higher values of V_s. However, there was a point of singular behavior for 50 mm/s, in connection with a change of trend in the shape of the laser tracks, mainly in terms of Rku. In addition, thanks to the micro-geometrical features of the textures under this processing condition, an increase in the HAZ thickness was achieved, giving the best results to generate intense and light tonalities.
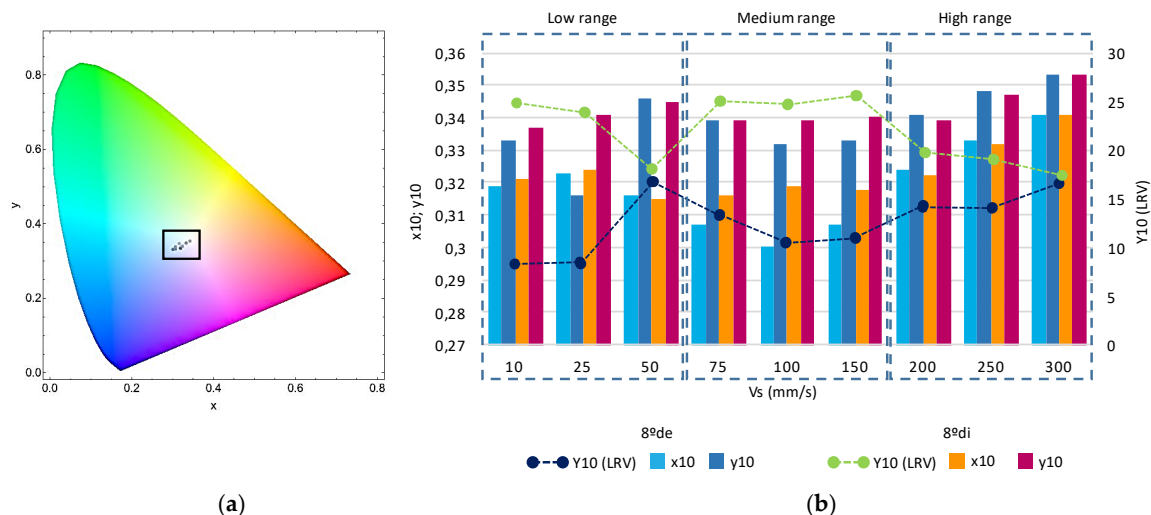

Figure 8. (**a**) Color chromaticity diagram of the textures (**b**) Color coordinate behavior as a function of V_s.

3.5. Reflectance and Optical Absorption of the Colored Titanium Surfaces

Most of the research about the reflectance of titanium alloys subjected to oxidative processes is focused on the development and analysis of continuous and flat surfaces. However, the possibility to incorporate additional properties by means of specific roughness topographies is shown as a gap in the study of these treatments. The sample color and reflectance shows an important dependency on the light incidence angle. This fact makes relevant the influence of surface finish on the optical properties of the textured Ti_6Al_4V substrates.

The LRVs of the samples showed that high scanning speeds produced a large effect on the reflectance of the titanium alloy. Interestingly, a similar effect was also observed at the low speed $V_s = 50$ mm/s. The difference between the LRVs obtained for the 8°/de and 8°/di optical geometries made clear the diffuse nature of the reflection for these samples and therefore the relation between the decrease observed in the LRVs and the increase of surface roughness.

Contrarily, LRVs for both low ($V_s = 10$ and 25 mm/s) and medium speeds showed a larger presence of the specular component in the total reflection of these samples, and thus a lower effect of the roughness in the reflectance of the samples.

On the other hand, the absorption spectra of the samples were derived from their corresponding reflection spectra, measured by the spectroscopic ellipsometer, and they are shown in Figure 9. A fitting model, which takes into account the surface roughness and the presence of an oxide layer on top of the titanium alloy, was used for the optical characterization of the samples. The Tauc–Lorentz dispersion model [29] was considered to model the optical constants (*n* and *k*) of the oxide layer. A significant increase in the absorption coefficient was found in the visible region for the scanning speeds in the medium range. These values stand out with respect to behavior found for the rest of the samples.
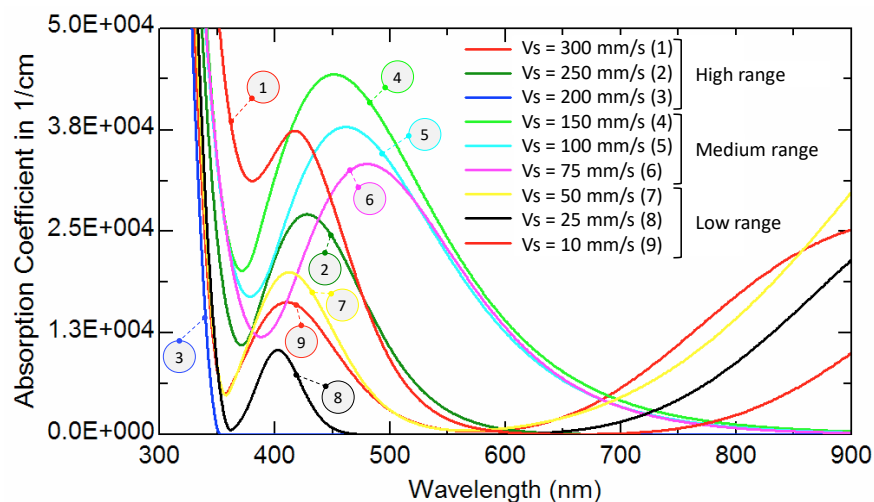

Figure 9. Absorption coefficient values of the laser textures.

4. Conclusions

In this research, specific topographies combined with color surfaces of titanium were obtained by changing the laser scanning speed in air atmosphere, using a fiber nanosecond pulsed laser. Experimental results confirm that the textured samples exhibit different roughness values combined with colorized surface, enhancing mechanical properties as hardness.

The development of the laser treatment in an atmospheric environment contributed to the generation of an oxide film on the surface of the alloy. Mainly due to the rapid heating and cooling stages, which are associated with pulsed laser irradiation, these treatments also affect the Ti6Al4V microstructure by transforming the closest areas of the laser tracks of the native surface to an α' martensite. A maximum area of higher than 4300 μm^2 on cross-sections of the textures and track depth as large as 174 μm were measured for the lowest scanning speed experiments (10 mm/s).

Extreme temperatures focused on small spot diameters, and the nature of cooling may have affected the formation of the oxide film and the phase transformation close to the tracks. This may be the cause of the existence in isolated cases of crack growth over the texturing channels in the most aggressive treatments (10 mm/s).

The existence of three scanning speed (V_s) ranges with clearly differentiated behaviors was verified for all the evaluated parameters. Samples treated with a lower range were characterized by deeper and narrow textured tracks with large heat-affected zones (HAZs) that induced important increases in hardness and lower absorption coefficient (α) values on near-blue/grey color surfaces.

Chromaticity values were located in a small ellipse on the center of the CIE 1931 color coordinate diagram for all texturing conditions used in the study. The main changes in optical properties of the textures were presented as an increase in the color coordinates (XYZ) and lightness (L*) as a function of the scanning speed of the beam. However, higher α values were detected in medium ranges of Vs. This suggests that the optically active film was strongly influenced by the depth and shape of the textures in addition to the thickness of the HAZ.

This combined topography/color texturing method provides a new methodology for the development of multi-functional surfaces, expanding the application range of materials and improving the performance of novel manufacturing processes.

Author Contributions: Conceptualization, J.M.V.-M., J.S. and J.M.G.-L.; Data curation, J.M.V.-M., J.S., E.B. and J.M.G.-L.; Formal analysis, J.S., E.B. and J.M.G.-L.; Investigation, J.M.V.-M.; Methodology, J.M.V.-M., E.B. and J.M.G.-L.; Writing – original draft, J.M.V.-M. and J.S.; Writing – review & editing, J.M.V.-M., J.S. and J.M.G.-L.

Conflicts of Interest: The authors declare no conflict of interest.

References

1. Etsion, I. State of the art in laser surface texturing. *J. Tribol. ASME Trans.* **2005**, *127*, 248–253. [CrossRef]

2. Salguero, J.; Del Sol, I.; Vazquez-Martinez, J.M.; Schertzer, M.; Iglesias, P. Effect of laser parameters on the tribological behavior of Ti6Al4V titanium microtextures under lubricated conditions. *Wear* **2019**, *426*, 1272–1279. [CrossRef]

3. Oh, J.M.; Lee, B.G.; Cho, S.W.; Choi, G.S.; Lim, J.W. Oxygen effects on the mechanical properties and lattice strain of Ti and Ti-6Al-4V. *Met. Mater. Int.* **2011**, *17*, 733–736. [CrossRef]

4. Bhaduri, D.; Batal, A.; Dimov, S.S.; Zhang, Z.; Dong, H.; Fallqvist, M.; Saoubid, R.M. On design and tribological behaviour of laser textured surfaces. *Procedia CIRP* **2017**, *60*, 20–25. [CrossRef]

5. James, A.S.; Thomas, K.; Mann, P.; Wall, R. The role and impacts of surface engineering in environmental design. *Mater. Des.* **2005**, *26*, 594–601. [CrossRef]

6. Ali, N.; Bashir, S.; Kalsoom, U.; Akram, M.; Mahmood, K. Effect of dry and wet ambient environment on the pulsed laser ablation of titanium. *Appl. Surf. Sci.* **2013**, *270*, 49–57. [CrossRef]

7. Drelich, J.; Chibowski, E.; Meng, D.D.; Terpilowski, K. Hydrophilic and superhydrophilic surfaces and materials. *Soft Matter* **2011**, *7*, 9804–9829. [CrossRef]

8. Pou, P.; Riveiro, A.; del Val, J.; Comesaña, R.; Penide, J.; Arias-González, F.; Soto, R.; Lusquiños, F.; Pou, J. Laser surface texturing of Titanium for bioengineering applications. *Procedia Manuf.* **2017**, *13*, 694–701. [CrossRef]

9. Mohammed, M.T.; Khan, Z.A.; Siddiquee, A.N. Surface modification of titanium materials for developing corrosion behavior in human body environment: A review. *Procedia Mater. Sci.* **2014**, *6*, 1610–1618. [CrossRef]

10. Vazquez-Martinez, J.M.; Salguero, J.; Botana, F.J.; Gomez-Parra, A.; Fernandez-Vidal, S.R.; Marcos, M. Tribological wear analysis of laser surface treated Ti6Al4V based on volume lost evaluation. *Key Eng. Mater.* **2014**, *615*, 82–87. [CrossRef]

11. Tian, Y.S.; Chen, C.Z.; Li, S.T.; Huo, Q.H. Research progress on laser surface modification of titanium alloys. *Appl. Surf. Sci.* **2005**, *242*, 177–184. [CrossRef]

12. Leuders, S.; Thone, M.; Riemer, A.; Niendorf, T.; Troster, T.; Richard, H.A.; Maier, H.J. On the mechanical behavior of titanium alloy Ti6Al4V manufactured by selective laser melting: Fatigue resistance and crack growth performance. *Int. J. Fatigue* **2013**, *48*, 300–307. [CrossRef]

13. Veiga, C.; Davim, J.P.; Loureiro, A.J.R. Properties and applications of titanium alloys: A brief review. *Rev. Adv. Mater. Sci.* **2012**, *32*, 133–148.

14. Patel, D.S.; Singh, A.; Balani, K.; Ramkumar, J. Topographical effects of laser surface texturing on various time-dependent wetting regimes in Ti6Al4V. *Surf. Coat. Technol.* **2018**, *349*, 816–829. [CrossRef]

15. Kümmel, D.; Hamman-Schroer, M.; Hetzner, H.; Schneider, J. Tribological behavior of nanosecond-laser surface textured Ti6Al4V. *Wear* **2019**, *422*, 261–268. [CrossRef]

16. Wen, M.; Wen, C.; Hodgson, P.; Li, Y. Thermal oxidation behavior of bulk titanium with nanocrystalline surface layer. *Corros. Sci.* **2012**, *59*, 352–359. [CrossRef]

17. Adams, D.P.; Murphy, R.D.; Saiz, D.J.; Hirschfeld, D.A.; Rodriguez, M.A.; Kotula, P.G.; Jared, B.H. Nanosecond pulsed laser irradiation of titanium: Oxide growth and effects on underlying metal. *Surf. Coat. Technol.* **2014**, *248*, 38–45. [CrossRef]

18. Alvarez, M.; Salguero, J.; Sánchez, J.A.; Huerta, M.; Marcos, M. SEM and EDS characterisation of layering TiOx growth onto the cutting tool surface in hard drilling processes of Ti-Al-V alloys. *Adv. Mat. Sci. Eng.* **2011**, *2011*, 414868.

19. Pérez del Pino, A.; Serra, P.; Morenza, J.L. Coloring of titanium by pulsed laser processing in air. *Thin Solid Film.* **2002**, *415*, 201–205. [CrossRef]

20. Pérez Del Pino, A.; Fernandez-Pradas, J.M.; Serra, P.; Morenza, J.L. Coloring of titanium through laser oxidation: Comparative study with anodizing. *Surf. Coat. Technol.* **2004**, *187*, 106–112. [CrossRef]

21. Vazquez-Martinez, J.M.; Salguero, J.; Botana, F.J.; Contreras, J.P.; Fernandez-Vidal, S.R.; Marcos, M. Metrological evaluation of the tribological behavior of laser surface treated Ti6Al4V alloy. *Procedia Eng.* **2013**, *63*, 752–760. [CrossRef]

22. Amara, E.H.; Haïd, F.; Noukaz, A. Experimental investigations on fiber laser color marking of steels. *Appl. Surf. Sci.* **2015**, *351*, 1–12. [CrossRef]

23. Vazquez-Martinez, J.M.; Del Sol, I.; Iglesias, P.; Salguero, J. Assessment the sliding wear behavior of laser microtexturing Ti6Al4V under wet conditions. *Coatings* **2019**, *9*, 67. [CrossRef]

24. Veiko, V.; Odintsova, G.; Ageev, E.; Karlagina, Y.; Loginov, A.; Skuratova, A.; Gorbunova, E. Controlled oxide films formation by nanosecond laser pulses for color marking. *Opt. Express* **2014**, *22*, 24342–24347. [CrossRef] [PubMed]

25. Vazquez-Martinez, J.M.; Botana, F.J.; Botana, M.; Salguero, J.; Marcos, M. Sliding wear behavior of UNS R56400 titanium alloy samples thermally oxidized by laser. *Materials* **2017**, *10*, 830. [CrossRef] [PubMed]

26. Grabowski, A.; Sozańska, M.; Adamiak, M.; Kępińska, M.; Florian, T. Laser surface texturing of Ti6Al4V alloy, stainless steel and aluminium silicon alloy. *Appl. Surf. Sci.* **2018**, *461*, 117–123. [CrossRef]

27. Gao, W.; Xue, Y.; Li, G.; Chang, C.; Li, B.; Hou, Z.; Li, K.; Wang, J. Investigations on the laser color marking of TC4. *Optik* **2019**, *182*, 11–18. [CrossRef]

28. Jwad, T.; Walker, M.; Dimov, S. Erasing and rewriting of titanium oxide colour marks using laser-induced reduction/oxidation. *Appl. Surf. Sci.* **2018**, *458*, 849–854. [CrossRef]

29. Jellison, G.E.; Modine, F.A. Parameterization of the optical functions of amorphous materials in the interband region. *Appl. Phys. Lett.* **1996**, *69*, 371–373. [CrossRef]

30. Pedeferri, M.P.; Del Curto, B.; Pedeferri, P. Chromatic properties of anodised titanium obtained with two techniques. In *Passivation of Metals and Semiconductors, and Properties of Thin Oxide Layers*; Elsevier: Amsterdam, The Netherlands, 2006; pp. 205–210.

31. Gupte, V.C. Expressing colours numerically. In *Colour Measurement Principles, Advances and Industrial Applications*; Elsevier: Amsterdam, The Netherlands, 2010; pp. 70–87.

32. *CIE 15:2004—Colorimetry*, 3rd ed.; International Commission on Illumination (CIE): Vienna, Austria, 2004.

33. *Light Reflectance Value (LRV) of a Surface—Method of Test*; BS 8493:2008+A1:2010; British Standard (BSI Group): London, UK, 2010.

34. *Geometrical Product Specifications (GPS)—Surface Texture: Profile Method—Terms, Definitions and Surface Texture Parameters*; International Organization Standardization (ISO): Geneva, Switzerland, 1997.

35. Yang, C.C.; Lin, Y.C.; Yang, C.C.; Lin, Y.H.; Huang, K.C.; Lin, K.M.; Hsiao, W.T. Laser-induced coloring of titanium alloy using ultraviolet nanosecond pulses scanning technology. *J. Alloys Compd.* **2017**, *715*, 349–361. [CrossRef]

36. Jwad, T.; Deng, S.; Butt, H.; Dimov, S. Laser induced single spot oxidation of titanium. *Appl. Surf. Sci.* **2016**, *387*, 617–624. [CrossRef]

37. Kosec, T.; Legat, A.; Kovač, J.; Klobčar, D. Influence of Laser Colour Marking on the Corrosion Properties of Low Alloyed Ti. *Coatings* **2019**, *9*, 375. [CrossRef]

38. Veiko, V.; Odintsova, G.; Gorbunova, E.; Ageev, E.; Shimko, A.; Karlagina, Y.; Andreeva, Y. Development of complete color palette based on spectrophotometric measurements of steel oxidation results for enhancement of color laser marking technology. *Mater. Des.* **2016**, *89*, 684–688. [CrossRef]